Magic Radio-Frequency Dressing of Nuclear Spins in High-Accuracy Optical Clocks

Thomas Zanon-Willette,[1,2,*] Emeric de Clercq,[3] and Ennio Arimondo[4]

[1]*UPMC Université Paris 06, UMR 7092, LPMAA, 4 place Jussieu, case 76, 75005 Paris, France*
[2]*CNRS, UMR 7092, LPMAA, 4 place Jussieu, case 76, 75005 Paris, France*
[3]*LNE-SYRTE, Observatoire de Paris, CNRS, UPMC, 61 avenue de l'Observatoire, 75014 Paris, France*
[4]*Dipartimento di Fisica "E. Fermi," Università di Pisa, Lgo. B. Pontecorvo 3, 56122 Pisa, Italy*

(Received 29 June 2012; published 30 November 2012)

A Zeeman-insensitive optical clock atomic transition is engineered when nuclear spins are dressed by a nonresonant radio-frequency field. For fermionic species as ^{87}Sr, ^{171}Yb, and ^{199}Hg, particular ratios between the radio-frequency driving amplitude and frequency lead to "magic" magnetic values where a net cancelation of the Zeeman clock shift and a complete reduction of first-order magnetic variations are produced within a relative uncertainty below the 10^{-18} level. An Autler-Townes continued fraction describing a semiclassical radio-frequency dressed spin is numerically computed and compared to an analytical quantum description including higher-order magnetic field corrections to the dressed energies.

DOI: 10.1103/PhysRevLett.109.223003 PACS numbers: 32.80.Qk, 06.30.Ft, 32.60.+i, 32.70.Jz

The interaction between magnetic fields and the nuclear or electronic magnetic moments represents a flexible tool for the control of the internal and external degrees of freedom in atoms or molecules, widely employed in precision measurements, frequency metrology, and coherent manipulations of quantum systems. In frequency metrology, the presence of magnetic fields may represent a limit on the realization of specific targets. In the attractive context of the "magic" wavelength combining a vanishing differential shift of the clock levels with the Lamb-Dicke regime greatly reducing the motional effects [1–3], the quest for magic magnetic field values where first-order Zeeman shift and magnetic fluctuation of the atomic transition are annulled, was proposed in Ref. [4] and studied experimentally in rubidium [5]. The best performances in optical clocks are accessible by using atomic transitions allowed by a weak hyperfine mixing mediated through a small spin-orbit coupling with a resolution at the millihertz level. To obtain even better performances, it has been proposed to use the bosonic even isotopes eliminating the nuclear spin and removing completely the first-order Zeeman effect with a residual second-order magnetic shift comparable to those of the ion standards [6]. However, in order to get rid of strong cold collision frequency shifts associated to the bosons, the present frequency metrology is concentrated on the fermionic species, such as ^{87}Sr [7–10], ^{171}Yb [11,12], and ^{199}Hg [13,14]. There, the first- and second-order Zeeman shifts contribute by 1 order of magnitude above the projected 10^{-18} fractional uncertainty of the frequency standard [7,9,10].

This Letter focuses on the atomic magnetic moment engineering with the target of getting rid of atomic properties sensitive to external electromagnetic fields. A scheme based on the radio-frequency (rf) quantum engineering of fermionic atomic states is presented in order to produce levels experiencing a vanishing first-order Zeeman clock shift. The cancelation of the first-order Zeeman shift applies also to the vectorial ac Stark shift, equivalent to an effective magnetic field, the only contribution of this kind appearing in ^{171}Yb and ^{199}Hg. The basic idea of letting a paramagnetic system mimic a nonmagnetic one originates from artificial or synthetic magnetism, where an atomic Hamiltonian is created by proper electromagnetic fields in order to simulate a given magnetic configuration [15]. Our work is inspired by the dressed-atom rf quantum engineering [16], where the paramagnetic response for two species, atoms in Ref. [17] or atom or neutron in Ref. [18], is tuned into the resonance.

The cancelation of the first-order Zeeman effect is produced by the atomic dressing at a rf frequency much larger than the effective Larmor precession, equivalent to a frequency modulation of the nuclear magnetization and a shielded nuclear response to the static magnetic field. The different rf response for the ground and excited states of the clock transition leads to crossing nodes in the energy diagram, where the atoms become nonmagnetic. This change from a paramagnetic system to an nonmagnetic one shares a strong analogy with a Landau theory of phase transition. In addition, at magic static field values the rf dressing engineers a Zeeman-insensitive atomic clock. This magic cancelation arises from the nonlinear magnetic Hamiltonian associated to the rf dressing of the two-electron system. Even if the dressing does not eliminate the second-order Zeeman contribution, its contribution to clock state separation is strongly decreased by an operation at a magic magnetic field. The stability of the ratio between rf dressing amplitude and rf angular frequency required to produce a target nonmagnetic state matched to the aimed optical clock accuracy is experimentally reachable. The present approach of a magic magnetic field cannot be applied to tensorial ac shifts.

For the alkali-earth atoms, a modified Breit-Wills theory describes the action of a magnetic field B producing linear

and quadratic nuclear spin-dependent Zeeman shifts for the doubly forbidden $|^1S_0\rangle \rightarrow |^3P_0\rangle$ optical clock transition [19]. For the $|F, m_F\rangle$ Zeeman level, the energy E_{m_F} is

$$E_{P,m_{F'}}(^3P_0) = m_{F'} g_P \mu_B B + \Delta_B^{(2)} B^2,$$
$$E_{S,m_F}(^1S_0) = m_F g_S \mu_B B, \quad (1)$$

where m'_F and m_F are the upper and lower magnetic quantum numbers, respectively, g_P and g_S the Landé g factors, with $g_P = g_S + \delta g$, and $\Delta_B^{(2)}$ the second-order Zeeman contribution, m_F independent. We will focus our attention on fermionic systems spin polarized in the extreme Zeeman sublevels [19,20], where a systematic average on the transition frequencies of optical transitions symmetrically placed around the line center is currently applied to cancel the linear Zeeman shift and to probe accurately the second-order Zeeman correction. Their parameters are listed in the Supplemental Material [21]. The Zeeman energies of the highest $|m_F|$ ^{87}Sr clock levels versus B are plotted in Fig. 1(a).

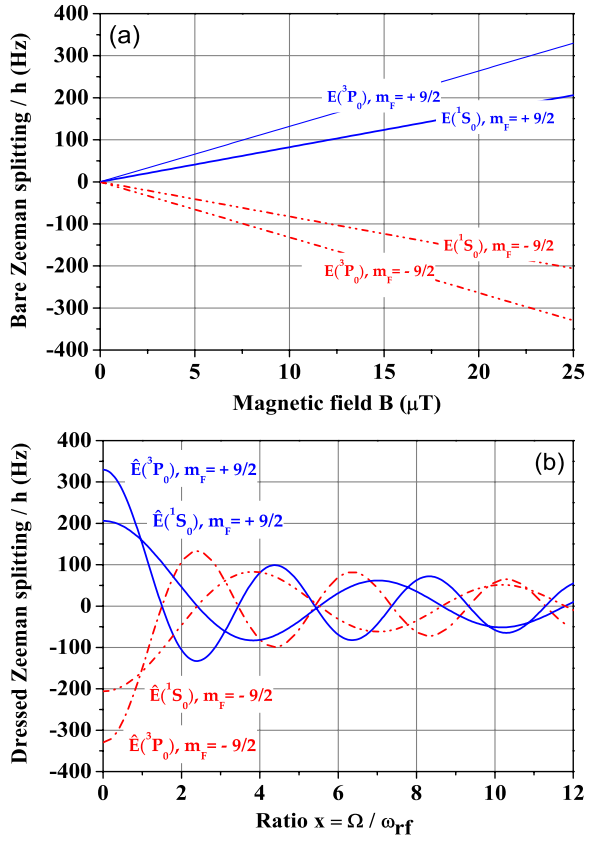

FIG. 1 (color online). (a) Bare Zeeman energy splitting E_{m_F} of the ^{87}Sr $|^1S_0; m_F = \pm 9/2\rangle$ and $|^3P_0; m_F = \pm 9/2\rangle$ clock states versus magnetic field B. (b) Dressed Zeeman energies $E^d_{m_F}$ ($^3P_0$, $^3S_0$) versus $x = \Omega/\omega_{\rm rf}$ at $\omega/2\pi = 2$ kHz and $B = 25$ μT. The crossing nodes with a zero first-order Zeeman shift determine the magic rf values.

We drive the clock atoms by a nonresonant rf field, linearly polarized and orthogonal to B, at angular frequency $\omega_{\rm rf}$ and (ground-state) Rabi frequency Ω; see Supplemental Material [21]. A strong modification of the Landé g factor occurs in the regime where $\mu_B B \ll \hbar\omega_{\rm rf}$. For dressing by a large number of rf photons, a perturbative quantum analysis predicts a dressed Landé g factor dependent on the zeroth-order Bessel function of the first kind $g_j^d(x_j) = g_j J_0(x_j)$, with $x_j = \Omega_j/\omega_{\rm rf}$, $\Omega_j = g_j\Omega/g_S$ ($j = P, S$) [22]. That dependence was verified in experiments on atoms [17,18,23], neutrons [24], and a chromium Bose-Einstein condensate [25]. It is valid for whatever spin value and equally spaced Zeeman levels [26]. When $\mu_B B \approx \hbar\omega_{\rm rf}$, the g_j^d expression includes an additional B dependence given by [26,27]

$$g_j^d = g_j\left[J_0(x_j) - \left(\frac{g_j\mu_B B}{\hbar\omega_{\rm rf}}\right)^2 S(x_j)\right], \quad (2)$$

$S(x)$ being a product of Bessel functions. However, for the first two crossing nodes of the rf dressed Zeeman energies of Fig. 1(b), the following approximated analytical $S(x)$ expression given by Ref. [28] provides the required accuracy:

$$S(x) = \frac{16}{2025x^4}[\alpha(x)J_2(x) + \beta(x)J_4(x) - \gamma(x)J_6(x)], \quad (3)$$

where functions are $\alpha(x) = 75(5x^2 - x^4/4)$, $\beta(x) = 6(408 - 74x^2 - 23x^4/16)$, and $\gamma(x) = 145(3x^2 - x^4/2)/49$. When the dressed Landé g factor of Eq. (2) is substituted into the energies of Eq. (1), the rf dressed energies contain both B^2 and B^3 nonlinear terms.

We derive the exact rf dressed Zeeman energies $E^d_{m_F}(j)$ from the Autler-Townes continued fraction

$$E^d_{m_F}(j) = E_{m_F}(j) + m_F\hbar\frac{\Omega}{2}\frac{g_j}{g_S}\cdot L(j). \quad (4)$$

The function L, representing the $m = 1/2$ dressed energy, normalized to the Rabi frequency [22], for a spin-1/2 system having ω_{21} energy splitting and rf dressed by a $\omega_{\rm rf}$ field with Rabi frequency Ω, is given by [29]

$$L = \cfrac{1}{L + \frac{4\omega_{21}}{\Omega}(1 - \frac{\omega_{\rm rf}}{\omega_{21}}) - \cfrac{1}{L - 8\frac{\omega_{21}}{\Omega}\frac{\omega_{\rm rf}}{\omega_{21}} - \frac{1}{L+\cdots}}}$$
$$+ \cfrac{1}{L + \frac{4\omega_{21}}{\Omega}(1 + \frac{\omega_{\rm rf}}{\omega_{21}}) - \cfrac{1}{L + 8\frac{\omega_{21}}{\Omega}\frac{\omega_{\rm rf}}{\omega_{21}} - \frac{1}{L+\cdots}}}. \quad (5)$$

The dressed nuclear Landé g factor is obtained by deriving the dressed energies with respect to B. Evaluation of dressed energies is done by retaining only a sufficient number of the quotients in each continued fraction needed to reach the desired accuracy. In practice, nine quotients are necessary.

The dressing field strongly modifies the Zeeman energies for each m_F clock state as shown in Fig. 1(b) for a

given static field B. The energies follow mainly the zero-order Bessel function dependence. The different $^1S_0$ and $^3P_0$ sensitivity to the dressing created by δg produces several crossings between the clock energies at particular $\Omega/\omega_{\rm rf}$ ratios. The dressed Zeeman clock shift

$$\Delta E^d_{m_F \to m'_F} = E^d_{m'_F}(^3P_0) - E^d_{m_F}(^1S_0) \tag{6}$$

is exactly compensated for by specific rf dressing parameters, for instance, in Fig. 2(a) at the $x = \Omega/\omega_{\rm rf} \approx 0.96$, 3.11, 5.44, ... for a π transition. The $\omega_{\rm rf}$ and Ω compensating values are determined by imposing the clock transition to be immune from the Zeeman shift, i.e., equal dressed magnetic energies.

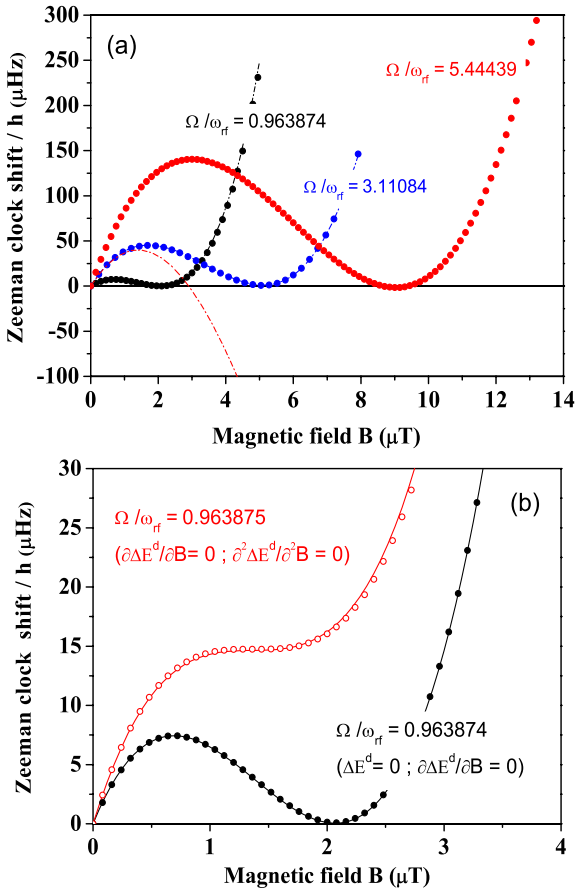

FIG. 2 (color online). ^{87}Sr dressed Zeeman shifts of the π clock transition ($m_F = -9/2$ or $m_F = 9/2$) versus B for $\omega_{\rm rf}/2\pi = 2$ kHz and the $\Omega/\omega_{\rm rf}$ values at, or around, the crossing nodes in Fig. 1. The curvature around the B values of the shift minima is the dressed second-order Zeeman shift. For the (b) open red data, the x is modified by one part in 10^6 from the crossing value to a value where the second-order Zeeman shift is annulled, in the presence of constant Zeeman bias. Open and closed dots are based on Eqs. (4) and (5), respectively. Lines based on Eqs. (2) and (3) are approximated solutions providing a good description around the first two crossing nodes only. 10 μHz corresponds to a 2×10^{-20} clock fractional shift.

A more ambitious target is to derive the magic fields where the pure-Zeeman differential shift is zero and also independent of the field value. That applies to the dressed Zeeman clock shift plotted in Fig. 2(a) with oscillations in the B dependence. At $\omega_{\rm rf}/2\pi = 2$ kHz and $\Omega/\omega_{\rm rf} = 0.963874$ we have a magic magnetic field value $B_m \approx 2.1$ μT which exactly cancels the full Zeeman shift for the $m_F = -9/2$, π transition, experiencing in addition a reduced $(B - B_m)^2$ sensitivity for the Zeeman energies. A reduction by 1 order of magnitude for that second-order sensitivity is obtained by operating close to the higher-order crossing nodes of Fig. 1(b), the first two also shown in Fig. 2(a) and corresponding to alternating $m_F = -9/2$ and $m_F = 9/2$ Zeeman sublevels. Figure 2(b) shows that, by changing the x parameter, a perfect cancelation of the $(B - B_m)^2$ magnetic sensitivity is reached, at the expense of a clock constant bias.

The magic (B_m, x_m) values where the Zeeman shift and the first-order sensitivity to weak field variations are simultaneously canceled are derived by imposing

$$\Delta E^d_{m_F \to m_{F'}}(x) = 0; \qquad \left(\frac{\partial \Delta E^d_{m_F \to m_{F'}}}{\partial B}\right)_x = 0. \tag{7}$$

The continued fraction solution of Eqs. (4) and (5) determines the magic values associated to the above conditions. Figure 3 reports the graphical approach applied to derive these magic B_m values. Notice that a suppression cannot be realized simultaneously for more than one m_F spin-dependent transition, because the B square dependence of Eq. (2) imposes for each optical transition a matched dressed g-factor compensation.

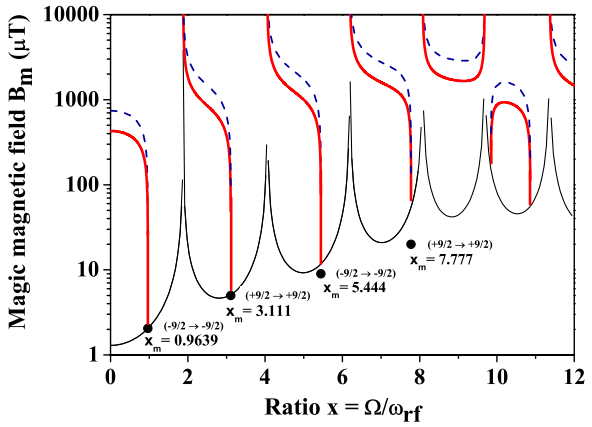

FIG. 3 (color online). (B, x) branches, derived from Eq. (7), defining a zero clock Zeeman shift $\Delta E^d = 0$ (thick solid red line) and a zero derivative $\partial \Delta E^d/\partial B = 0$ (dashed blue line) for the alternating $m_F = -9/2$ and $m_F = 9/2$ π clock transitions in ^{87}Sr. Their intersections determine the (B_m, x_m) magic values also denoted by the solid dots from a numerical evaluation of Eqs. (4) and (5). The thin solid black line dependence reports the $B(x)$ of Eq. (8), but magic B_m values occur only at magic x_m parameters. All curves are for $\omega_{\rm rf}/2\pi = 2$ kHz.

TABLE I. Magic (x_m, B_m) pairs for π and $\sigma^{\pm}$ ^{87}Sr, ^{171}Yb, and ^{199}Hg optical clock transitions based on Eqs. (4) and (5), at fixed $\omega_{\rm rf}/2\pi = 2$ kHz. The $x_m = \Omega_m/\omega_{\rm rf}$ values are reported here with the experimental accuracy of the Landé factor, but a fractional shift below 10^{-19} requires a six-digit resolution.

		^{87}Sr		
$m_F \to m_{F'}$	$-\frac{9}{2} \to -\frac{9}{2}$	$+\frac{9}{2} \to +\frac{9}{2}$	$-\frac{9}{2} \to -\frac{9}{2}$	$+\frac{9}{2} \to +\frac{9}{2}$
x_m	0.9639	3.111	5.444	7.777
B_m (μT)	2.1	5.1	9.0	20.0
		^{171}Yb		
$m_F \to m_{F'}$	$+\frac{1}{2} \to +\frac{1}{2}$	$-\frac{1}{2} \to -\frac{1}{2}$	$+\frac{1}{2} \to +\frac{1}{2}$	$-\frac{1}{2} \to -\frac{1}{2}$
x_m	0.9776	3.157	5.527	7.906
B_m (μT)	0.08	0.12	0.33	0.68
$m_F \to m_{F'}$	$-\frac{1}{2} \to +\frac{1}{2}$	$+\frac{1}{2} \to -\frac{1}{2}$	$-\frac{1}{2} \to +\frac{1}{2}$	$+\frac{1}{2} \to -\frac{1}{2}$
x_m	1.826	4.107	5.543	6.954
B_m (μT)	0.11	0.59	0.88	0.82
		^{199}Hg		
$m_F \to m_{F'}$	$+\frac{1}{2} \to +\frac{1}{2}$	$-\frac{1}{2} \to -\frac{1}{2}$	$+\frac{1}{2} \to +\frac{1}{2}$	$-\frac{1}{2} \to -\frac{1}{2}$
x_m	0.9115	2.931	5.117	7.221
B_m (μT)	0.02	0.05	0.11	0.34
$m_F \to m_{F'}$	$-\frac{1}{2} \to +\frac{1}{2}$	$+\frac{1}{2} \to -\frac{1}{2}$	$-\frac{1}{2} \to +\frac{1}{2}$	$+\frac{1}{2} \to -\frac{1}{2}$
x_m	1.674	3.599	4.566	6.388
B_m (μT)	0.04	0.19	0.17	0.16

As a good approximation, calculating the dressed energies through the effective Landé g factor of Eq. (2) we get the following expression of the magic B_m field as a function of the $\omega_{\rm rf}$ and x_m parameters:

$$B_m(\omega_{\rm rf}, x_m) = \frac{\hbar^3 \omega_{\rm rf}^2 \Delta_B^{(2)}/(2\mu_B^3)}{m_{F'} g_P^3 S\left(\frac{g_P}{g_S} x_m\right) - m_F g_S^3 S(x_m)}. \quad (8)$$

Table I reports at fixed $\omega_{\rm rf}$ few magic pairs (x_m, B_m), at increasing B_m values, for the π polarization atomic clock of the fermionic species of present interest. The $\omega_{\rm rf}/2\pi = 2$ kHz choice, producing a consistent table for all the fermionic atoms, leads to very small magic field values for the mercury atom. Higher values, more easily manageable in the laboratory, are simply obtained by increasing the rf frequency and applying the Eq. (8) scaling. The accuracy of the dressed energy and the magic pairs strongly depends on the atomic parameters as tested by a numerical evaluation of the continued fraction. A complete "full-scale" calculation as reported in Refs. [4,30] would be required for accurate magic numerical values including all the digits recommended for a correct evaluation. To highlight the resolution which should be targeted for canceling the Zeeman shifts below the 10^{-19} level, we have used a six-digit resolution for figures when necessary.

The magic field values are calculated at a fixed $\Omega/\omega_{\rm rf}$ value that implies a very large precision in the setting of the Ω and $\omega_{\rm rf}$ parameters. For a practical application, the stability of those quantities becomes an important issue. While a very high stability of the rf frequency is not a problem, the Ω accuracy could be an issue. We have explored the Ω stability required in the operation of an optical clock, and the results are reported in Fig. 4. A change in Ω, or precisely a change in x by one part in ten thousand, corresponds to a fractional shift of the optical clock at the 10^{-17} level. In order to reach the ultimate limit of the alkali-earth optical clocks [1], because only the x ratio of the rf quantities is important for the rf engineering, the Ω variations may be compensated for by acting on the rf frequency. Thus, a feedback on the rf frequency should reach the required ratio stability, in order to reach a 10^{-20}

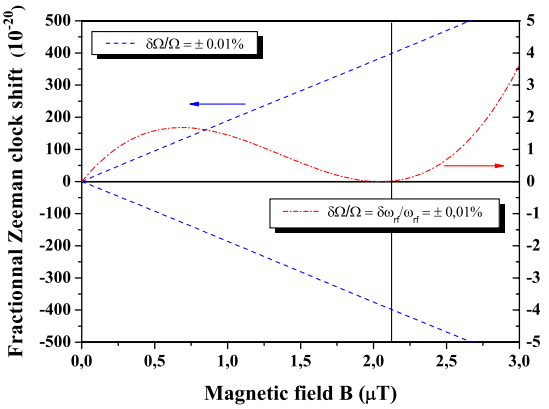

FIG. 4 (color online). Fractional clock shift, measured in 10^{-20} relative units, for the ^{87}Sr $m_F = -9/2$ π transition, for a rf amplitude fluctuation by 0.01% (left scale) and for correlated variations of the same amount applied to both amplitude and rf frequency (right scale). Operating point $x_{\rm rf} = 0.96\ldots$ and $\omega_{\rm rf}/2\pi = 2$ kHz, leading to the magic $B = 2.1$ μT value.

level in Fig. 4. In practice, the rf stability could be matched to the actual accuracy of the optical clock. For large ω_{rf} excursions, the efficiency of this compensation is limited by the ω_{rf}^2 dependence in the B_m numerator of Eq. (8).

We have verified that the shift produced by virtual transitions induced by the rf field between the ^3P fine structure levels is negligible compared to the finally aimed clock accuracy. The presence of vectorial ac shift contribution to the atomic energies introduces an additional shift of the clock levels. When the ac shift is comparable to the Zeeman shift, the key features of the rf dressing, crossing nodes, compensations of the clock shift, and magic values, are obtained also for this case, with magic (x_m, B_m) pairs depending on the specific ac shift. Schemes for the rf compensation of the ac tensorial part appearing in the ^{87}Sr optical clock only should be investigated.

The combination of well-engineered optical-trapping potential and of rf quantum engineering represents an important tool in the investigation of alkali-earth clock systematics. We have verified our scheme feasibility within the operation regime of the present optical clocks. The averaging over the Zeeman components of the optical clock transition is directly performed by the rf dressing of the atomic system. For an implementation within an optical lattice where magnetic fields are created synthetically [15], the dressing magnetic field may be originated by the rf modulation of the lattice depth, at least for frequencies low enough for an atomic adiabatic following.

The synthetic rf controlled magnetism may be applied to other atomic or molecular and solid-state physics configurations. Besides compensating the residual Zeeman contribution to a superstable optical clock based on a nuclear transition [31], the rf engineering may be applied to design an artificial quantum transition with specific Zeeman properties, as a two-level superconducting system driven by an oscillatory field [32], and to the control of spin coherent dynamics and transport in semiconductor systems [33,34].

The authors thank S. Bize, M. Glass-Maujean, A. Godone, C. Janssen, B. Laburthe-Tolra, R. Le Targat, A. D. Ludlow, and J. Ye for their inputs at different stages of this work. E. A. was supported by a MIUR PRIN-2009 grant.

*thomas.zanon@upmc.fr

[1] J. Ye, H. J. Kimble, and H. Katori, Science **320**, 1734 (2008).
[2] H. Katori, Nat. Photonics **5**, 203 (2011).
[3] A. Derevianko and H. Katori, Rev. Mod. Phys. **83**, 331 (2011).
[4] A. Derevianko, Phys. Rev. A **81**, 051606(R) (2010).
[5] R. Chicireanu, K. Nelson, S. Olmschenk, N. Lundblad, A. Derevianko, and J. Porto, Phys. Rev. Lett. **106**, 063002 (2011).
[6] A. V. Taichenachev, V. Yudin, C. Oates, C. Hoyt, Z. Barber, and L. Hollberg, Phys. Rev. Lett. **96**, 083001 (2006).
[7] A. D. Ludlow *et al.*, Science **319**, 1805 (2008).
[8] P. G. Westergaard, J. Lodewyck, L. Lorini, A. Lecallier, E. Burt, M. Zawada, J. Millo, and P. Lemonde, Phys. Rev. Lett. **106**, 210801 (2011).
[9] A. Yamaguchi, M. Fujieda, M. Kumagai, H. Hachisu, S. Nagano, Y. Li, T. Ido, T. Takano, M. Takamoto, and H. Katori, Appl. Phys. Express **4**, 082203 (2011).
[10] St. Falke *et al.*, Metrologia **48**, 399 (2011).
[11] Z. W. Barber *et al.*, Phys. Rev. Lett. **100**, 103002 (2008).
[12] N. D. Lemke, A. Ludlow, Z. Barber, T. Fortier, S. Diddams, Y. Jiang, S. Jefferts, T. Heavner, T. Parker, and C. Oates, Phys. Rev. Lett. **103**, 063001 (2009).
[13] H. Hachisu, K. Miyagishi, S. Porsev, A. Derevianko, V. Ovsiannikov, V. Pal'chikov, M. Takamoto, and H. Katori, Phys. Rev. Lett. **100**, 053001 (2008).
[14] L. Yi, S. Mejri, J. J. McFerran, Y. L. Coq, and S. Bize, Phys. Rev. Lett. **106**, 073005 (2011).
[15] J. Dalibard, F. Gerbier, G. Juzeliünas, and P. Öhberg, Rev. Mod. Phys. **83**, 1523 (2011).
[16] C. Cohen-Tannoudji and D. Guery-Odelin, *Advances in Atomic Physics: An Overview* (World Scientific, Singapore, 2011).
[17] S. Haroche and C. Cohen-Tannoudji, Phys. Rev. Lett. **24**, 974 (1970).
[18] A. Esler, J. Peng, D. Chandler, D. Howell, S. Lamoreaux, C. Liu, and J. Torgerson, Phys. Rev. C **76**, 051302(R) (2007); P.-H. Chu *et al.*, *ibid.* **84**, 022501(R) (2011).
[19] M. M. Boyd, T. Zelevinsky, A. Ludlow, S. Blatt, T. Zanon-Willette, S. Foreman, and J. Ye, Phys. Rev. A **76**, 022510 (2007).
[20] X. Baillard *et al.*, Eur. Phys. J. D **48**, 11 (2008).
[21] See Supplemental Material at http://link.aps.org/supplemental/10.1103/PhysRevLett.109.223003 for the values of the Landé g-factors and second-order Zeeman effect.
[22] Notice that owing to the different Landé g factor in the ground and excited states, the $^3P_0$ Rabi frequency is $g_P\Omega/g_S$.
[23] S. Haroche, C. Cohen-Tannoudji, C. Audoin, and J. P. Schermann, Phys. Rev. Lett. **24**, 861 (1970).
[24] E. Muskat, D. Dubbers, and O. Schärpf, Phys. Rev. Lett. **58**, 2047 (1987).
[25] Q. Beaufils, T. Zanon, R. Chicireanu, B. Laburthe-Tolra, E. Maréchal, L. Vernac, J.-C. Keller, and O. Gorceix, Phys. Rev. A **78**, 051603(R) (2008).
[26] G. W. Series, Phys. Rep. **43**, 1 (1978).
[27] C. Cohen-Tannoudji, J. Dupont-Roc, and C. Fabre, J. Phys. B **6**, L218 (1973); P. Hannaford, D. T. Pegg, and G. W. Series, *ibid.* **6**, L222 (1973).
[28] F. Ahmad and R. K. Bullough, J. Phys. B **7**, L275 (1974).
[29] S. H. Autler and C. H. Townes, Phys. Rev. **100**, 703 (1955).
[30] P. Rosenbusch, S. Ghezali, V. Dzuba, V. Flambaum, K. Beloy, and A. Derevianko, Phys. Rev. A **79**, 013404 (2009).
[31] C. J. Campbell, A. Radnaev, A. Kuzmich, V. Dzuba, V. Flambaum, and A. Derevianko, Phys. Rev. Lett. **108**, 120802 (2012).
[32] J. Tuorila, M. Silveri, M. Sillanpää, E. Thuneberg, Y. Makhlin, and P. Hakonen, Phys. Rev. Lett. **105**, 257003 (2010).
[33] S. Q. Shen, Phys. Rev. Lett. **95**, 187203 (2005).
[34] J. Ohe, M. Yamamoto, T. Ohtsuki, and J. Nitta, Phys. Rev. B **72**, 041308(R) (2005).